16th International Conference on Greenhouse Gas Control Technologies, GHGT-16

23rd -27th October 2022, Lyon, France

Experimental measurements and thermodynamic modeling of CO_2 solubility in the NaCl-Na_2SO_4-$CaCl_2$-$MgCl_2$ system up to 150 °C and 200 bar

P.F. dos Santos[a], H. Messabeb[a], M. Ducousso[a], F. Contamine[a], P. Cézac[a], A. Lassin[b], L. André[b,c,1]

[a] *Université de Pau et des Pays de l'Adour/ E2S UPPA, Laboratoire de Thermique, Energétique et Procédés - IPRA, EA1932, 64000, Pau, France*

[b] *BRGM – 3 avenue C. Guillemin – 45000 Orléans, France*

[c] *Univ. Orléans, CNRS, BRGM, ISTO UMR 7327, F – 45071 Orleans, France*

Abstract

To face the climate change, the geological storage of CO_2 in deep saline aquifers has been gaining interest. This study investigates the CO_2 solubility in single-salt solutions containing NaCl, Na_2SO_4, $CaCl_2$ and $MgCl_2$. In a first part, an experimental campaign has been performed in an instrumented batch reactor. Acid-base and conductimetric titrations were performed. CO_2 solubility points were obtained for pressure and temperature up to 20 MPa and 423.15 K. The salting-out effect has been studied (at a same ionic force of 3 mol/kg) showing the following order: $SO_{\%,CaCl_2} < SO_{\%,MgCl_2} < SO_{\%,NaCl} < SO_{\%,Na_2SO_4}$. In parallel to laboratory experiments, a modelling work has been carried out to calculate the gas solubility. The specific numerical tool named PhreeSCALE was used. The activity coefficient has been calculated using the Pitzer formalism. Interaction parameters for the CO_2-H_2O-$MgCl_2$ and CO_2-H_2O-$CaCl_2$ systems were optimized successfully.

Keywords: CO_2 solubility, single-salt and mixed-salt solutions, thermodynamic modeling, activity coefficient

1. Introduction

CO_2 Capture and Storage in deep geological formation (CCS) is taking part of the panel of possibilities (in addition to the development of renewable energies) to reduce emissions of greenhouse gases to the atmosphere. To develop the CCS field, it is important to predict the quantity of CO_2 that could be stored in the reservoirs [1,2]. Geochemical models are able to predict the solubility of CO_2 in geological formations, which is directly dependent on the brine composition, its temperature and pressure conditions. These models are also supported by the constant acquisition of new experimental data to reinforce databases [3–5]. Many studies have been dedicated to the solubility of CO_2 in pure water. As far as single-salt solution are concerned, the CO_2-H_2O-NaCl system is the most investigated with more than 1500 solubility points published for pressures up to 140 MPa, temperatures comprised between 273,15-723,15 K and molalities up to 6 mol/kg. In a much lesser extent, some studies are dedicated to other salts such as $CaCl_2$, Na_2SO_4 and $MgCl_2$. To our knowledge, 450 and 400 solubility points are available regarding the CO_2-H_2O-

[1]* Corresponding author. Email *address:* l.andre@brgm.fr

$CaCl_2$ and CO_2-H_2O-Na_2SO_4 systems, respectively. The CO_2-H_2O-$MgCl_2$ system at high pressure, temperature and salinity has been mostly studied by 3 groups [6–8].

Several thermodynamic models have been proposed to calculate the solubility of CO_2 in pure water and in aqueous brine solutions [9–11]. Among them, the Pitzer model is highly successful to compute the activity coefficients in aqueous solutions rich in dissolved salts. Several authors worked on developing activity coefficient expressions for specific electrolytic systems and for specific operational conditions [11–13]. However, there are still gaps in their ability to cover a wide range of temperatures and chemical compositions of aqueous brines that are encountered in natural deep media targeted for CO_2 geological storage applications. These gaps mainly concerned CO_2 solubility in single-salt systems containing either Na_2SO_4, $CaCl_2$ or $MgCl_2$ electrolytes near salt saturation, and in salt mixtures.

This study focuses on improving the geochemical modeling of electrolytic systems containing NaCl, $CaCl_2$, Na_2SO_4 and/or $MgCl_2$. In a first part, the objective was to generate experimental data on CO_2 solubility in single-salt solutions over a temperature range consistent with the conditions of the targeted storage reservoirs [323,15-423,15 K], for pressures up to 20 MPa and in different salt concentrations [1 to 5 mol/kg]. A discussion of the salting-out effect is also proposed. In a second part, we report the development of a model to calculate the CO_2 solubility in electrolytic single-salt solutions of $CaCl_2$ and $MgCl_2$ and in a mixed-salt solution with temperatures up to 473,15 K, pressures up to 40 MPa and salt concentrations near saturation. The Pitzer formalism has been applied due to the high salinity of the solutions. A new set of interaction parameters has been generated to accurately described CO_2 solubility in electrolytic solutions near saturation. All the calculations were performed with the PhreeSCALE geochemical simulation software, which allows calculating the CO_2 solubility using an activity-fugacity approach [14].

2. Material and methods

2.1. *Experimental set-up, chemicals and protocol*

The names of the compounds, their respective CAS registration numbers, as well as the source and purity of the chemicals used in our work are summarized in Table 1.

Table 1: list of chemicals used in this study.

Chemical name	**Formula**	**N° CAS**	**Source**	**Purity**
Carbon dioxide	CO_2	124-38-9	Air Liquide	99.7 %wt
Magnesium chloride hexahydrate	$MgCl_2.6H_2O$	7791-18-6	VWR	100% wt
Sodium Chloride	NaCl	7647-14-5	Acros Organics	99%
Sodium hydroxide	NaOH	1310-73-2	Fisher Scientific	46/51 %wt
Calcium chloride	$CaCl_2$	10043-52-4	Acros Organics	96%
Hydrochloric acid	HCl	7647-01-0	VWR	0.1 ± 2 % mol/L
Pure water	H_2O	7732-18-5	Barnstead Smart2Pure system	18.2 MΩ.cm

The acquisition of new CO_2 solubility data is carried out on an experimental laboratory pilot, consisting mainly of a Hastelloy C276 autoclave with a volume of 1 L thermostatically controlled (see Fig.1). It can operate at temperatures between 293,15 and 473,15 K. CO_2 loading in the autoclave is performed using a thermostated volumetric pump (Top Industrie PMHP 200-200), which could operate for a pressure up to 20 MPa and offers automatic pressure compensation after each sampling. Details on the reactor description can be found in a previous publication [15].

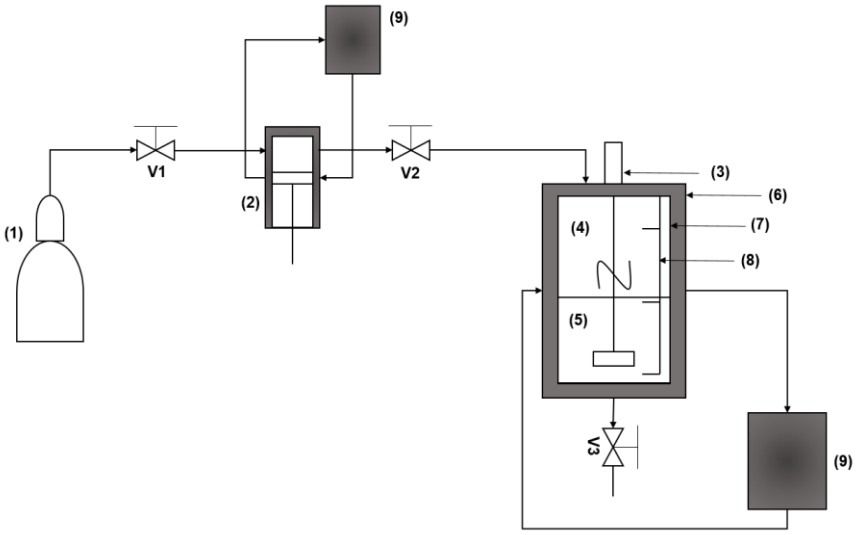

Fig. 1. Scheme of the experimental cell. (1) CO_2 bottle; (2) thermostatic volumetric pump; (3) stirrer; (4) gas phase; (5) aqueous phase; (6) autoclave in Hastelloy C276; (7) double jacket; (8) thermocouples; and (9) thermostatic baths [15].

2.2. *Operating procedure*

Before manipulation, the reactor, the lines and the pump are purged and put under vacuum (see Fig.1). The liquid solution is injected by aspiration, the temperature is set, and the carbon dioxide charged to the desired temperature through the valve V3. Stirring is activated at a speed of 800 RPM. The pressure in the reactor decreases because of the dissolution of CO_2 in the liquid phase. To compensate the pressure drop, the valve V2 is open and then closed again (once the target pressure is reached). Once pressure and temperature equilibrate, agitation is maintained for about one hour (minimum) to ensure the thermodynamic equilibrium of the system. For sampling, a syringe containing a precisely known quantity of sodium hydroxide is connected to the autoclave (valve V3). The valve V3 of the autoclave is open to take aqueous saturated samples. The mass of the sample is obtained by weighing the syringe before and after the end of the sampling. Sodium hydroxide must always be in excess to ensure the total conversion of CO_2 and HCO_3^- into CO_3^{2-}, according to reactions (1) and (2), to prevent any outgassing before analysis.

$$CO_{2(g)} + 2\ OH^-_{(aq)} \leftrightarrow\ CO_3^{2-}{}_{(aq)} + H_2O_{(l)} \quad (1)$$

$$HCO_3^-{}_{(aq)} + OH^-{}_{(aq)} \leftrightarrow\ CO_3^{2-}{}_{(aq)} + H_2O_{(l)} \quad (2)$$

The total dissolved inorganic carbon is quantified by titration (see Section 2.3).

For the CO_2-H_2O-$MgCl_2$ system, because the salt dissolved in the aqueous phase will react with the soda as shown in reaction (3), the excess sodium hydroxide must be sufficient to ensure reactions (1), (2) and (3) are complete:

$$MgCl_{2(aq)} + 2\ NaOH_{(aq)} \leftrightarrow Mg(OH)_{2(aq)} + 2\ NaCl_{(aq)} \quad (3)$$

As far as the CO_2-H_2O-$CaCl_2$ system is concerned, carbonate ions will directly precipitate with calcium ones to form calcium carbonate:

$$CO_3^{2-} + Ca^{2+} \leftrightarrow CaCO_{3(s)} \quad (4)$$

2.3. *Chemical analysis*

The measurements of carbon dioxide solubility is made by an automatic titrator using a pH electrode coupled to a conductimetric titration. Contents of the syringe are dosed with 0.1 M hydrochloric acid solution. The measured chemical species present in the syringe are the OH^- and CO_3^{2-} ions. From the titration curve, three equivalence points can be detected, as shown in the Figure 2.a. The first equivalence point (V_1) corresponds to the neutralization of the excess of NaOH in the sample, as shown in reaction (5), although it is not always visible. The second equivalence point (V_2) corresponds to the conversion of CO_3^{2-} into HCO_3^-(reaction 6). Finally, the V_3 equivalence point corresponds to the transformation of HCO_3^- into H_2CO_3 (reaction 7), which is equivalent to $CO_{2(aq)} + H_2O$.

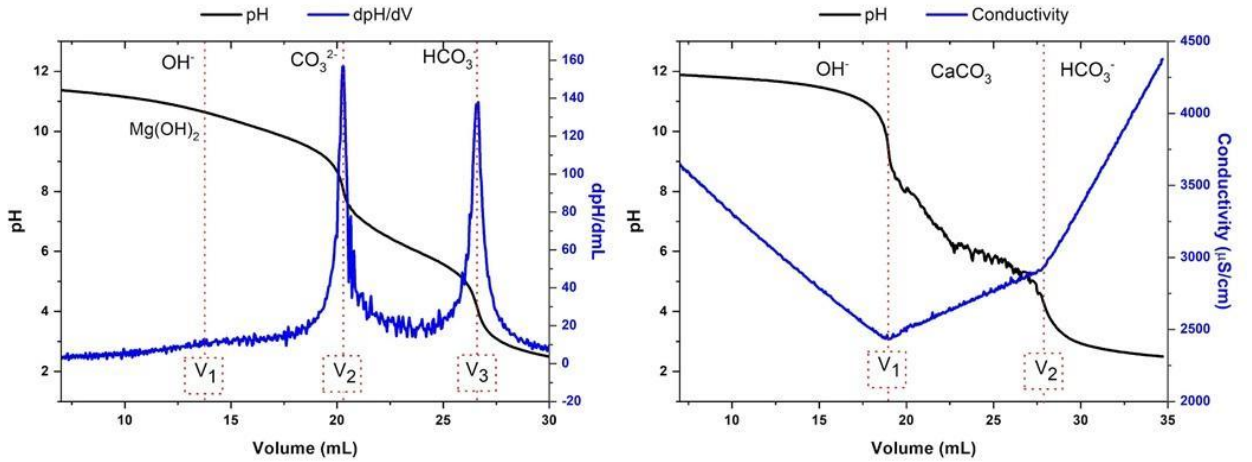

Fig. 2. a) Example of pH and dpH/dV curve *vs* volume of hydrochloric solution added, b) example of pH and conductivity curves *vs* volume of hydrochloric solution added.

$$OH^-_{(aq)} + H^+_{(aq)} \leftrightarrow H_2O_{(l)} \quad (5)$$

$$CO_3^{2-}{}_{(aq)} + H^+_{(aq)} \leftrightarrow HCO_3^-{}_{(aq)} \quad (6)$$

$$HCO_3^-{}_{(aq)} + H^+_{(aq)} \leftrightarrow H_2CO_{3(aq)} \quad (7)$$

Then, the amount of moles of CO_2 can be determined and checked according to the following expression:

$$\eta_{CO_2} = \eta_{CO_3^{2-}} = \eta_{HCO_3^-} = \frac{C_{HCl}\,(V_3 - V_2)}{1000} \quad (8)$$

As far as the CO_2-H_2O-$CaCl_2$ system is concerned, the conductimetric signal is utilized to calculate the CO_2 solubility. The pH signal is recorded to ensure results but is not enough precise. An example of conductimetric result is shown in Fig. 2b. The first part characterized by a decrease of conductivity corresponds to the neutralization of the excess of soda in the sample. The first equivalent point is encountered at the end of this step, where the pH value is around 9. Then, the addition of acid titrant leads to the dissolution of the carbonate precipitate. This is indicated by the second part of the graph, where the conductivity of the solution slightly increases from volume V_1. The second end-point (V_2) is reached when the precipitate is totally dissolved following the reaction:

$$CaCO_{3(s)} + 2H^+_{(aq)} \leftrightarrow Ca^{2+}{}_{(aq)} + H_2CO_{3(aq)} \quad (9)$$

The results reported in this work are the means of five successive titrations performed under each set of equilibrium conditions. To ensure that our sampling process is valid, some criteria have been set, making it easier to identify and exclude possible bad analyzes. These criteria are described elsewhere [3,15].

2.4. *Experimental uncertainty*

The experimental uncertainty of the present work was evaluated by the analysis of variances (ANOVA) that consists of a statistical method based on repeatability and reproducibility experiments. The principle of the ANOVA methodology was applied and discussed in previous papers [8,15]. The uncertainty was obtained from the analysis of three different experiments (evaluation of reproducibility) performed under the same conditions with five titrations for each experiment (evaluation of repeatability).

3. Experimental results

Fig.3 presents the molality of CO_2 versus pressure (0 to 20 MPa) for pure water and single-salt solutions of NaCl, $CaCl_2$, $MgCl_2$ and Na_2SO_4 at a temperature of 323,15 K and a salt molality of 1 mol/kg. All curves behaviors are similar: an important solubility increase along with pressure up to 10 MPa and then a plateau. The CO_2 solutility is the highest for pure water. The second highest solubility is obtained for the NaCl solution while the lowest one is obtained for the Na_2SO_4 one. It illustrates the salting-out effect which corresponds to a decrease of gas solubility when increasing the salinity of a solution. Several studies investigated this phenomenon and highlighted that the salting-out effect depends on the type of electrolyte, its concentration, the temperature and the pressure. However, there is still a lack of understanding.

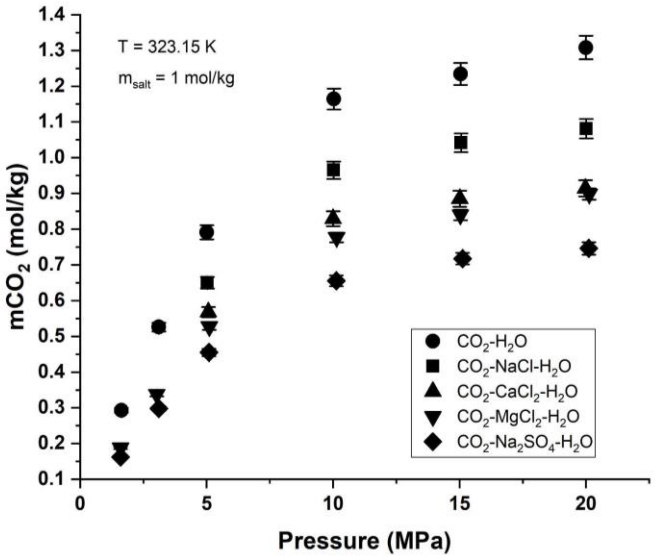

Fig. 3: CO_2 molality versus pressure for pure water and the single-salt aqueous solutions of NaCl, $CaCl_2$, $MgCl_2$ and Na_2SO_4 at 323,15 K and 1 mol/kg of salt.

Koschel et al., 2006 [16] defined the salting-out effect ($SO_{\%}$) as the calculation of the relative difference between the solubility of gas (here carbon dioxide) in saline solutions (m) and the solubility of the same gas in pure water (m^0) under the same conditions of temperature and pressure (Eq.10) :

$$SO_{\%} = \frac{100 \times (m^0 - m)}{m^0} \quad (10)$$

Fig.4 presents all the CO_2 solubility data for the NaCl, $CaCl_2$, $MgCl_2$ and Na_2SO_4 solutions obtained by the LaTEP for ionic strength of 3 mol/kg, temperatures of 323, 373 and 423 K; a range of pressure of 5, 10, 15 and 20 MPa. A total of 48 solubility points are gathered including our previous results [3,8,15,17]. This figure allows us to compare directly the salting-out effect of $CaCl_2$, $MgCl_2$ and Na_2SO_4 versus NaCl. It is possible to observe the following order: $SO_{\%,CaCl_2} < SO_{\%,MgCl_2} < SO_{\%,NaCl} < SO_{\%,Na_2SO_4}$. As it has been discussed in the literature, it is possible to observe that a divalent cation presents a higher salting-out effect than a monovalent one. Regarding the anions, SO_4^{2-} seems to be more impacting on the CO_2 solubility than the Cl^- ion. Hence, the same conclusion as for cations could be done, which is in accordance with Tong et al., 2013 [7]. The charge density of the ion has been also presented as an important parameter [6,8]. In Fig. 4, one can observe that $MgCl_2$ presents a bigger salting-out effect than $CaCl_2$ and it is known that the charge density of Mg^{2+} is higher than the one of Ca^{2+}, the ionic radius of Mg being smaller than that of Ca. At equal valency, an anion with a higher charge density will present a higher salting-out effect. It has also been observed by Zhao et al., 2015 [6].

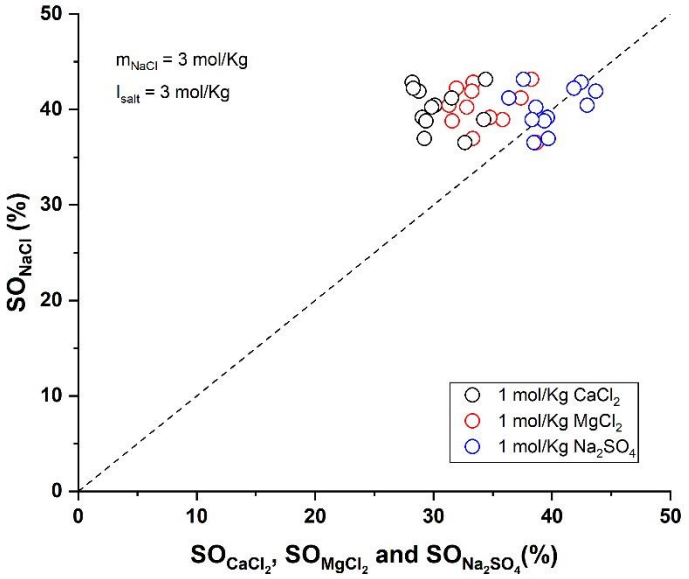

Fig. 4. Comparison of the salting-out effect between the CO_2-H_2O-NaCl [17], CO_2-H_2O-$CaCl_2$ [3], CO_2-H_2O-Na_2SO_4 [15] and CO_2-H_2O-$MgCl_2$ [8] at ionic force of 3 mol/kg.

4. Thermodynamic Modeling

4.1. Thermodynamic approach γ-φ

The geochemical calculation code PhreeSCALE allows calculating the CO_2 solubility. It relies on a dissymmetrical approach γ-φ [18]:

$$m_{CO_2} = \frac{\varphi_{CO_2}^{vap} \times P \times y_{CO_2}}{\gamma_{CO_2}^{m}} \times K_H \times \exp\left(\frac{-V_{m,CO_2}(P - P_0)}{RT}\right)\frac{m_0}{P_0} \quad (11)$$

Where m_{CO_2} is the molality (mol/kg), K_H the Henry's law constant (molality scale), V_{m,CO_2} the molar volume at infinite dilution (cm^3/mol), y_{CO_2} the molar fraction (mol/mol) in the gas phase and $\varphi_{CO_2}^{vap}$ which is the fugacity coefficient (unitless) calculated with the Peng-Robinson equation of state. R is the ideal gas constant (8.314 J/mol K),

P is the pressure (bar) and T is the temperature (K). The subscript 0 represents the standard state, P_0 is equal to 1 atm, and m_0 to 1 mol/kg.

$\gamma^{m}_{CO_2}$ is the activity coefficient (molality scale) described by the Pitzer formalism [19]. This model explicitly accounts for temperature, species molality and their respective molecular interactions:

$$\ln\left(\gamma^{m}_{CO_2}\right) = 2m_{CO_2}\lambda_{CO_2,CO_2} + \sum_{c=1}^{n_C} 2m_c\lambda_{CO_2,c} + \sum_{a=1}^{n_a} 2m_a\lambda_{CO_2,a} + \sum_{c=1}^{n_C}\sum_{a=1}^{n_a} m_c m_a \zeta_{CO_2,c,a} \quad (12)$$

λ and ζ are binary and ternary interaction parameters, respectively. c and a stand for cations and anions, respectively. Binary and ternary interaction parameters can be described as a function of temperature (Y can be any of the adjustable specific interaction parameter) by the following expression (which is a combination of equations of Christov and Møller, 2004 and Møller, 1988) as proposed by Lach et al., 2016 [14]:

$$Y(T) = A1 + A2.T + A3.T^2 + A4.T^3 + \frac{A5}{T} + A6.\ln T + \frac{A7}{(T-263)} + \frac{A8}{(680-T)} + \frac{A9}{(T-227)} \quad (13)$$

Practically, as few coefficients as possible are used in this equation.

4.2. Determination of interaction parameters

First, the interaction parameters for CO_2-H_2O, CO_2-H_2O-NaCl and CO_2-H_2O-Na_2SO_4 systems were optimized and addressed in a previous publication [18]. The model generated through these parameters is capable of reproducing with great precision the experimental data available in the literature [18] over a wide range of $P-T-m_{salt}$ conditions (namely, 273,15–473,15 K, 0,1–40 MPa and 0–6 mol/kg). Then, taking advantage of these parameters, the interaction parameters for systems containing salt of the $CaCl_2$ and $MgCl_2$ type were investigated individually. For the CO_2-H_2O-$CaCl_2$ system, the solubility data from Messabeb et al., 2017 [3] were used ($P-T-m_{salt}$ range of 323,15–423,15 K, 5–20 MPa and 1–3–6 mol/kg), totaling 36 experimental points. For the CO_2-H_2O-$MgCl_2$ system, the 33 data points published by dos Santos et al., 2021 [8] were used ($P-T-m_{salt}$ range of 323,15–423,15 K, 1,5–20 MPa and 1–3–5 mol/kg).

The optimizations were performed by coupling PhreeSCALE with PEST [22] according to the principle described in [23]. PhreeSCALE calculates the solubility of CO_2, using an initial set of values for the specific interaction parameters to be estimated. These calculated results are then compared with the experimental CO_2 solubility values by calculating the objective function that characterizes the deviation with respect to the experimental data. The process is repeated automatically with a new set of interaction parameters until the convergence criteria is satisfied through the method of successive iterations.

4.3. Data analysis calculations

In addition to a graphical evaluation, the average absolute deviations (AAD) between the proposed model ($m^{cal}_{CO_2,i}$) and the experimental data of CO_2 solubility ($m^{exp}_{CO_2,i}$) were also calculated according to Eq. 14:

$$AAD_{\%} = \frac{100}{Np}\sum_{i=1}^{Np}\left(\left|\frac{m^{cal}_{CO_2,i} - m^{exp}_{CO_2,i}}{m^{exp}_{CO_2,i}}\right|\right) \quad (14)$$

The calculated deviations are shown in Tables 3 and 4.

5. Modeling Results and discussions

5.1. Parameterization

For the CO_2-H_2O-$CaCl_2$ system, the parameterization had to comply with the recent work of Lassin et al. [24] where the partial dissociation of the $CaCl_2$ electrolyte in the $CaCl_2$-H_2O binary system is considered. Consequently, interaction parameters were determined for interactions between CO_2 and the species Ca^{2+}, $CaCl^+$ and $CaCl_2^0$. In the CO_2-H_2O-$MgCl_2$ system, the parameters were obtained for interactions between the CO_2 and Mg^{2+} species. The parameterization results are reported in Table 2.

Table 2. Pitzer interaction parameters and coefficients for the temperature dependent polynomial of the Eq. (13) after the optimization.

	A_1	**A_2**	**A_3**	**A_4**	**A_5**	**$A_{6...}A_9$**	**Reference**
λ_{CO_2,Cl^-}	0	0	0	0	0	0	[18]
$\lambda_{CO_2,Ca^{2+}}$	1.457807316	-1.45E-03	0	0	-258.1444166	0	This study
$\lambda_{CO_2,CaCl^+}$	-4.055035906	5.84E-03	0	0	708.62675080	0	This study
$\lambda_{CO_2,CaCl_2^0}$	0	0	0	0	0	0	This study
$\lambda_{CO_2,Mg^{2+}}$	0.5259193460	-1.87E-03	2.60E-06	0	0	0	This study
$\zeta_{CO_2,Ca^{2+},Cl^-}$	0	0	0	0	0	0	This study
$\zeta_{CO_2,CaCl^+,Cl^-}$	0	0	0	0	0	0	This study
$\zeta_{CO_2,CaCl_2^0,Cl^-}$	0	0	0	0	0	0	This study
$\zeta_{CO_2,Mg^{2+},Cl^-}$	-0.01	0	0	0	0	0	This study

In the CO_2-H_2O-$MgCl_2$ system, only the binary interaction parameters were used in a first attempt, in order to minimize the number of parameters. However, without the ternary parameters, the differences between the simulations and experimental data for systems concentrated in salt were large. Thus, the ternary parameter $\zeta_{CO_2,Mg^{2+},Cl^-}$ was added as a constant to improve the capacity of the model, as previously work [18]. As for the CO_2-H_2O-$CaCl_2$ system, only the temperature dependence was sufficient. Such differences can be attributed to different representations of the binary chemical systems: full dissociation of $MgCl_2$ versus partial dissociation of $CaCl_2$.

5.2. CO_2-H_2O-Ca^{2+}-Cl^- system

Once the new Pitzer interaction parameters were established for the CO_2-H_2O-$CaCl_2$ system, simulations and graphical comparisons were performed. Figures 5a and 5b show that the isothermal solubilities of CO_2 in the aqueous solutions of $CaCl_2$ calculated by the model are in agreement with the experimental data at 373 and 423 K. Although the interaction parameters of Pitzer were obtained at pressures between 5 and 20 MPa, the figures show that the model is also able to reproduce correctly the solubility data for pressures below 5 MPa and above 20 MPa.

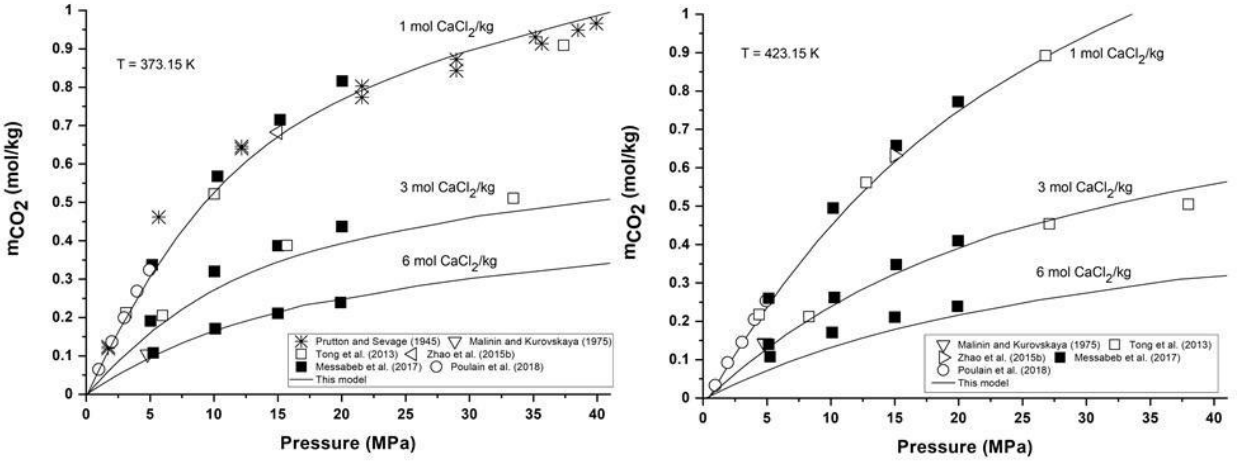

Fig. 5. CO_2 solubilities in aqueous $CaCl_2$ solution calculated by PhreeSCALE (solid lines) vs. experimental data (symbols) [3,6,7,25–27] a) at 373.15K and b) at 423.15 K.

The model for $CaCl_2$ was also tested for different temperatures and concentrations. Nearly 370 experimental data from the literature were compared, with an overall mean absolute difference close to 7%. Thus, the proposed model is able to cover a wide range of $P - T - m_{CaCl_2}$ (293,15-424 K, 0,1-40 MPa and 0-6,3 mol/kg). Overall, the model is capable of reproducing with good quality much of the experimental data present in the literature. However, it is worth noting that several studies have inconsistencies regarding the repeatability of the data [25,28], in addition to error bars or non-existent or greater than 15%, as [29,30].

Table 3. Calculated deviations of CO_2 solubility in aqueous $CaCl_2$ and $MgCl_2$ solutions. Np is the number of experimental data.

References	**T (K)**	**P (MPa)**	**m$CaCl_2$ (mol/kg)**	**Np**	**AAD (%)**
[25]	348-394	1.5-67.3	1-3.9	115	5.82
[31]	293-323	4.795	0.441-4.495	10	8.25
[31]	373-423	4.795	1.1-6.3	10	11.52
[32]	298-308	0.1	0.22-5.3	16	7.96
[33]	318.15	2.09-15.86	1	8	8.55
[7]	309-424	1.53-37.9	1-5.0	36	8.31
[29]	328.15-375.15	6.89-20.69	1.9-4.8	22	6.49
[6]	323-423	15	0.333-2	18	2.45
[28]	302-338	0.28-11.7	0.1-1	25	8.34
[3]	323.15-423.15	5.0-20	0.1-6.0	36	5.16
[30]	323.15-373.15	5-15.3	0.74-1.94	8	11.81
[34]	323.15-423.15	6.5-59.7	0.7306-2.7526	43	5.60
[27]	323-423	1.2-5.0	1	15	3.61
[4]	323-333	6-40.0	0.2-1	6	2.18
Overall				**368**	**6.86**
References	**T (K)**	**P (MPa)**	**m$MgCl_2$ (mol/Kg)**	**Np**	**AAD (%)**
[32]	288.15-308.15	0.1	0.328-3.012	21	2.15
[7]	309.52-424.63	1.25-31.2	1-5.0	39	6.76
[6]	323-423	15	0.333-2	18	1.88
[34]	323.15-423.15	8.23-54.48	0.754-4.29	35	2.62
[8]	323.15-423.15	1.5-20	1-3.0	33	2.21
Overall				**146**	**3.13**

5.3. CO_2-H_2O-Mg^{2+}-Cl^- system

Experimental studies of CO_2 solubility data in systems containing magnesium chloride are rare for varied ranges of pressure, temperature and salt concentration. This rarity also extends to thermodynamic modeling works on this system. Three studies, based on the activity coefficient model of Pitzer, propose binary and ternary interaction parameters[6,11,35].

Fig. 6a and 6b show that the simulations carried out with Pitzer interaction parameters determined from experimental data acquired in this work, are also able to represent correctly data from other experimental studies [6,7]. It is at note that Tong et al., 2013 [7] also measured CO_2 solubility at pressures greater than 20 MPa (at 373 K) and that our model remains suitable in these conditions.

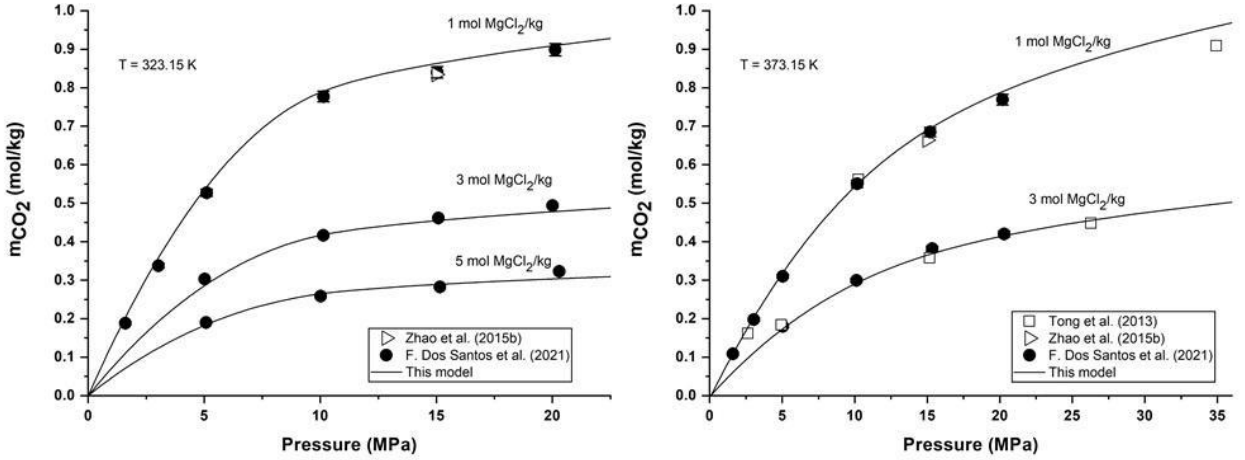

Fig. 6. CO_2 solubilities in aqueous $CaCl_2$ solution calculated by PhreeSCALE (solid lines) vs. experimental data (symbols) [6–8].

Table 3 presents the results of the mean absolute deviations (AAD) between our model and the different CO_2 solubility data in $MgCl_2$ aqueous solutions. The calculations were made on one hundred and forty-six experimental data published in the literature. The model as a whole presents an AAD of 3.13% compared to the experimental data. For all the authors studied, except [7], the model had mean absolute discrepancies less than 3%. Data from Tong et al., 2013 [7] at 5 mol/kg show experimental errors that can vary between 1 and 10%; the presented AAD of 6.76% resides in the experimental errors presented by the author. Thus, the model is capable of covering a wide range of $P - T - m_{MgCl_2}$, 288-424 K, 0,1-54,5 MPa and 0-5 mol/kg.

Our model was also compared to the 35 experimental points by Mousavi Belfeh Teymouri, 2017 [34] who obtained solubility data for pressures greater than 20 MPa (up to 54 MPa). Most of the data points are therefore outside of the pressure range considered for model optimization and yet, the AAD obtained is less than 2.7%. This shows the robustness of our model and its extensibility to pressures greater than 20 MPa.

5.4. CO_2-Na^+-Ca^{2+}-Cl^--H_2O system

As a continuation of our work to model CO_2 solubility in pure water and single salt systems (CO_2-H_2O-NaCl, CO_2-H_2O-Na_2SO_4, CO_2-H_2O-$CaCl_2$ and CO_2-H_2O-$MgCl_2$), we focused on complex chemical systems containing salt

mixtures. In the case of the CO_2-H_2O-NaCl-Na_2SO_4 system, CO_2 solubility data were measured and compared t²o the model, leading to AAD values of less than 4% [18].

Table 4. Calculated deviations of CO_2 solubility in aqueous NaCl-$CaCl_2$ solutions. Np is the number of experimental data.

References	T (K)	P (MPa)	mNaCl (mol/kg)	mCaCl₂ (mol/kg)	Np	AAD (%)
[33]	318.15	2.46-16.02	0.951	0.505	8	11.06
[6]	323 - 423	15	1.06 - 2.9856	0.217-0.666	24	2.85
[5]	323 - 423	1.2-5.0	1.2	0.2	24	2.47
[4]	333 - 453	6-40.0	1.2	0.2	10	2.29
Overall					**66**	**4.67**

Ultimately, the model was also tested on the CO_2-H_2O-NaCl-$CaCl_2$ system, using data collected in the literature. Table 4 shows that the model satisfactorily reproduces the data presented by [4,5,36]. More specifically, Figures 7a and 7b illustrate the comparison between the model and the data from [5] and [4], respectively.

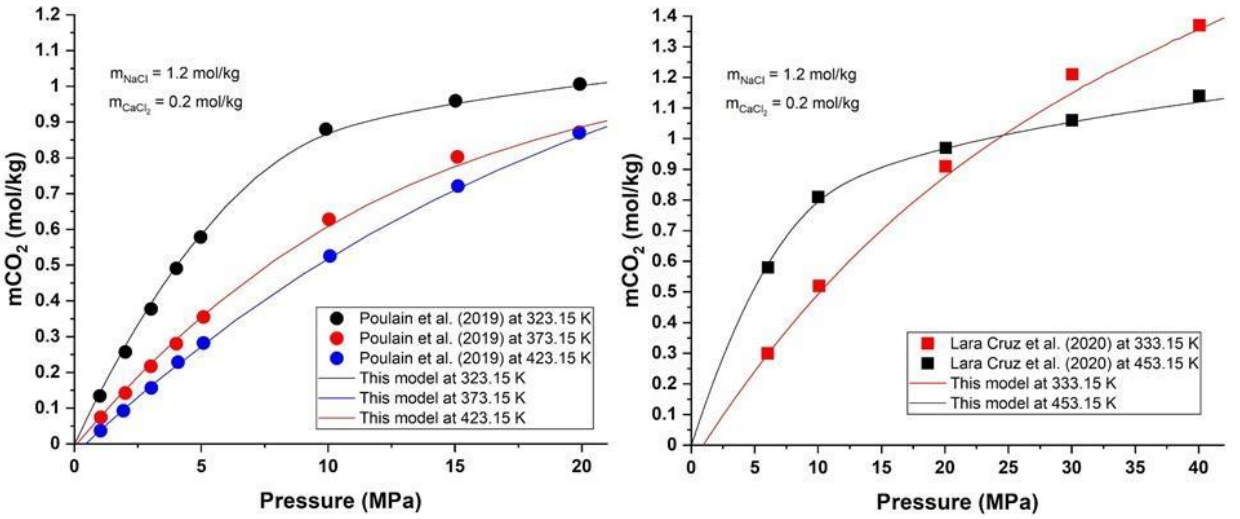

Fig. 7. CO_2 solubilities in aqueous NaCl-$CaCl_2$ solution calculated by PhreeSCALE (solid lines) vs. experimental data (symbols) [4,5].

6. Conclusions

This study gathers experimental data of CO_2 solubility in NaCl, Na_2SO_4, $CaCl_2$ and $MgCl_2$ aqueous solutions. Various concentrations were considered, up to salt solubilities; the temperature ranged from 303 K to 423 K and the pressure ranged from 1.5 to 20 MPa. The salting-out effect has been studied (at a same ionic force of 3 mol/kg) showing the following order: $SO_{\%,CaCl_2} < SO_{\%,MgCl_2} < SO_{\%,NaCl} < SO_{\%,Na_2SO_4}$. In parallel to laboratory experiments and a bibliographic data collection, a modeling work has been carried out to calculate the gas solubility. The specific numerical tool named PhreeSCALE was used to calculate activity coefficients according to the Pitzer formalism. Interaction parameters for the CO_2-H_2O-$MgCl_2$ and CO_2-H_2O-$CaCl_2$ systems were optimized. CO_2 solubility in these two systems, as well as in the mixed-salt system (1,2 mol/kg NaCl and 0,2 mol/kg $CaCl_2$) could be modelled successfully. Comparison to the literature results in overall AAD smaller than 10% and shows the extrapolation capabilities of the model.

References

[1] T. Torp, J. Gale, Demonstrating Storage of CO_2 in Geological ReservoirsThe Sleipner and Sacs Projects, in: Greenh. Gas Control Technol. - 6th Int. Conf., Elsevier, 2003: pp. 311–316. https://doi.org/10.1016/B978-008044276-1/50050-7.

[2] S.M. Benson, D.R. Cole, CO_2 sequestration in deep sedimentary formations, Elements. 4 (2008) 325–331. https://doi.org/10.2113/gselements.4.5.325.

[3] H. Messabeb, F. Contamine, P. Cézac, J.P. Serin, C. Pouget, E.C. Gaucher, Experimental Measurement of CO_2 Solubility in Aqueous $CaCl_2$ Solution at Temperature from 323.15 to 423.15 K and Pressure up to 20 MPa Using the Conductometric Titration, J. Chem. Eng. Data. 62 (2017) 4228–4234. https://doi.org/10.1021/acs.jced.7b00591.

[4] J. Lara Cruz, E. Neyrolles, F. Contamine, P. Cézac, Experimental Study of Carbon Dioxide Solubility in Sodium Chloride and Calcium Chloride Brines at 333.15 and 453.15 K for Pressures up to 40 MPa, J. Chem. Eng. Data. (2020) acs.jced.0c00592. https://doi.org/10.1021/acs.jced.0c00592.

[5] M. Poulain, H. Messabeb, A. Lach, F. Contamine, P. Cézac, J.-P. Serin, J.-C. Dupin, H. Martinez, Experimental Measurements of Carbon Dioxide Solubility in Na–Ca–K–Cl Solutions at High Temperatures and Pressures up to 20 MPa, J. Chem. Eng. Data. 64 (2019) 2497–2503. https://doi.org/10.1021/acs.jced.9b00023.

[6] H. Zhao, R.M. Dilmore, S.N. Lvov, Experimental studies and modeling of CO_2 solubility in high temperature aqueous $CaCl_2$, $MgCl_2$, Na_2SO_4, and KCl solutions, AIChE J. 61 (2015) 2286–2297. https://doi.org/10.1002/aic.14825.

[7] D. Tong, J.P.M. Trusler, D. Vega-Maza, Solubility of CO_2 in Aqueous Solutions of $CaCl_2$ or $MgCl_2$ and in a Synthetic Formation Brine at Temperatures up to 423 K and Pressures up to 40 MPa, J. Chem. Eng. Data. 58 (2013) 2116–2124. https://doi.org/10.1021/je400396s.

[8] P. F. dos Santos, L. André, M. Ducousso, F. Contamine, P. Cézac, Experimental Measurements of CO_2 Solubility in Aqueous $MgCl_2$ Solution at Temperature between 323.15 and 423.15 K and Pressure up to 20 MPa, J. Chem. Eng. Data. (2021). https://doi.org/10.1021/acs.jced.1c00347.

[9] R.D. Springer, Z. Wang, A. Anderko, P. Wang, A.R. Felmy, A thermodynamic model for predicting mineral reactivity in supercritical carbon dioxide: I. Phase behavior of carbon dioxide–water–chloride salt systems across the H_2O-rich to the CO_2-rich regions, Chem. Geol. 322–323 (2012) 151–171. https://doi.org/10.1016/j.chemgeo.2012.07.008.

[10] Z. Duan, R. Sun, C. Zhu, I.M. Chou, An improved model for the calculation of CO_2 solubility in aqueous solutions containing Na^+, K^+, Ca^{2+}, Mg^{2+}, Cl^-, and SO_4^{2-}, Mar. Chem. 98 (2006) 131–139. https://doi.org/10.1016/j.marchem.2005.09.001.

[11] X. Shi, S. Mao, An improved model for CO_2 solubility in aqueous electrolyte solution containing Na+, K+, Mg^{2+}, Ca^{2+}, Cl^- and SO_4^{2-} under conditions of CO_2 capture and sequestration, Chem. Geol. 463 (2017) 12–28. https://doi.org/10.1016/j.chemgeo.2017.05.005.

[12] D. Li, Z. Duan, The speciation equilibrium coupling with phase equilibrium in the H_2O–CO_2–NaCl system from 0 to 250 C, from 0 to 1000 bar, and from 0 to 5 molality of NaCl, Chem. Geol. (2007).

[13] S. Mao, D. Zhang, Y. Li, N. Liu, An improved model for calculating CO_2 solubility in aqueous NaCl solutions and the application to CO_2–H_2O–NaCl fluid inclusions, Chem. Geol. 347 (2013) 43–58. https://doi.org/10.1016/j.chemgeo.2013.03.010.

[14] A. Lach, F. Boulahya, L. André, A. Lassin, M. Azaroual, J.-P. Serin, P. Cézac, Thermal and volumetric properties of complex aqueous electrolyte solutions using the Pitzer formalism – The PhreeSCALE code, Comput. Geosci. 92 (2016) 58–69. https://doi.org/10.1016/j.cageo.2016.03.016.

[15] P.F. dos Santos, L. André, M. Ducousso, F. Contamine, P. Cézac, Experimental Measurement of CO_2 Solubility in Aqueous Na_2SO_4 Solution at Temperatures between 303.15 and 423.15 K and Pressures up to 20 MPa, J. Chem. Eng. Data. 65 (2020) 3230–3239. https://doi.org/10.1021/acs.jced.0c00230.

[16] D. Koschel, J.-Y. Coxam, L. Rodier, V. Majer, Enthalpy and solubility data of CO_2 in water and $NaCl_{(aq)}$ at conditions of interest for geological sequestration, Fluid Phase Equilib. 247 (2006) 107–120. https://doi.org/10.1016/j.fluid.2006.06.006.

[17] H. Messabeb, F. Contamine, P. Cézac, J.P. Serin, E.C. Gaucher, Experimental Measurement of CO_2 Solubility in Aqueous NaCl Solution at Temperature from 323.15 to 423.15 K and Pressure of up to 20 MPa, J. Chem.

Eng. Data. 61 (2016) 3573–3584. https://doi.org/10.1021/acs.jced.6b00505.

[18] P.F. dos Santos, L. Andre, M. Ducousso, A. Lassin, F. Contamine, A. Lach, M. Parmentier, P. Cézac, An improved model for CO_2 solubility in aqueous Na^+–Cl^-–SO_4^{2-} systems up to 473.15 K and 40 MPa, Chem. Geol. (2021) 120443. https://doi.org/10.1016/j.chemgeo.2021.120443.

[19] K.S. Pitzer, Activity coefficients in electrolyte solutions, CRC press, 1991.

[20] N. Møller, The prediction of mineral solubilities in natural waters: A chemical equilibrium model for the Na-Ca-Cl-SO_4-H_2O system, to high temperature and concentration, Geochim. Cosmochim. Acta. 52 (1988) 821–837. https://doi.org/10.1016/0016-7037(88)90354-7.

[21] C. Christov, N. Møller, Chemical equilibrium model of solution behavior and solubility in the H-Na-K-OH-Cl-HSO_4-SO_4-H_2O system to high concentration and temperature, Geochim. Cosmochim. Acta. 68 (2004) 1309–1331. https://doi.org/10.1016/j.gca.2003.08.017.

[22] J. Doherty, PEST: Model-Independent Parameter Estimation, 5th ed., (2004).

[23] L. André, A. Lassin, M. Azaroual, A methodology to estimate Pitzer interaction parameters, Geochim. Cosmochim. Acta Suppl. 73 (2009) A41.

[24] A. Lassin, L. André, A revised description of the binary $CaCl_2$-H_2O chemical system up to solution-mineral equilibria and temperatures of 250°C using Pitzer equations. Extension to the multicomponent HCl-LiCl-NaCl-KCl-$MgCl_2$-$CaCl_2$-H_2O system, J. Chem. Thermodyn. (n.d.).

[25] C.F. Prutton, R.L. Savage, The Solubility of Carbon Dioxide in Calcium Chloride-Water Solutions at 75, 100, 120° and High Pressures 1, J. Am. Chem. Soc. 67 (1945) 1550–1554. https://doi.org/10.1021/ja01225a047.

[26] S.D. Malinin, N.A. Kurovskaya, Investigation of CO_2 solubility in solution of chlorides at elevated temperature and pressures of CO_2, Geochemistry Int. (1975).

[27] M. Poulain, M. Poulain, H. Messabeb, F. Contamine, P. Cézac, J.P. Serin, J.C. Dupin, H. Martinez, Experimental Measurement of CO_2 Solubility in a 1 mol/kg_w $CaCl_2$ Solution at Temperature from 323.15 to 423.15 K and Pressure up to 20 MPa, in: Cutting-Edge Technol. Carbon Capture, Util. Storage, John Wiley & Sons, Inc., Hoboken, NJ, USA, 2018: pp. 123–134. https://doi.org/10.1002/9781119363804.ch9.

[28] K. Gilbert, P.C. Bennett, W. Wolfe, T. Zhang, K.D. Romanak, CO_2 solubility in aqueous solutions containing Na^+, Ca^{2+}, Cl^-, SO_4^{2-} and HCO_3^-: The effects of electrostricted water and ion hydration thermodynamics, Appl. Geochemistry. 67 (2016) 59–67. https://doi.org/10.1016/j.apgeochem.2016.02.002.

[29] A. Bastami, M. Allahgholi, P. Pourafshary, Experimental and modelling study of the solubility of CO_2 in various $CaCl_2$ solutions at different temperatures and pressures, Pet. Sci. 11 (2014) 569–577. https://doi.org/10.1007/s12182-014-0373-1.

[30] B. Liborio, Dissolution du dioxyde de carbone dans des solutions aqueuses d'électrolyte dans le contexte du stockage géologique: Approche thermodynamique (French Ph.D. Thesis), Université Clermont Auvergne, 2017.

[31] S.D. Malinin, N.I. Saveleva., Experimental investigations of CO2 solubility in NaCl and CaCl2 solutions at temperatures of 25, 50 and 75 degrees and elevated CO_2 pressure., Geochemistry Int. (1972).

[32] A. Yasunishi, F. Yoshida, Solubility of carbon dioxide in aqueous electrolyte solutions, J. Chem. Eng. Data. 24 (1979) 11–14. https://doi.org/10.1021/je60080a007.

[33] Y. Liu, M. Hou, G. Yang, B. Han, Solubility of CO_2 in aqueous solutions of NaCl, KCl, $CaCl_2$ and their mixed salts at different temperatures and pressures, J. Supercrit. Fluids. 56 (2011) 125–129. https://doi.org/10.1016/j.supflu.2010.12.003.

[34] S.R. Mousavi Belfeh Teymouri, Phase equilibria measurements and modelling of CO_2-rich fluids/brine systems, Heriot-Watt University, 2017.

[35] X. Sun, Z. Wang, H. Li, H. He, B. Sun, A simple model for the prediction of mutual solubility in CO_2-brine system at geological conditions, Desalination. 504 (2021) 114972. https://doi.org/10.1016/j.desal.2021.114972.

[36] H. Zhao, R. Dilmore, D.E. Allen, S.W. Hedges, Y. Soong, S.N. Lvov, Measurement and Modeling of CO_2 Solubility in Natural and Synthetic Formation Brines for CO_2 Sequestration, Environ. Sci. Technol. 49 (2015) 1972–1980. https://doi.org/10.1021/es505550a.